Cement and Concrete Composites 111 (2020) 103621

Contents lists available at ScienceDirect

Cement and Concrete Composites

journal homepage: http://www.elsevier.com/locate/cemconcomp

Effect of the source concrete with ASR degradation on the mechanical and physical properties of coarse recycled aggregate

M. Barreto Santos [a], J. de Brito [b,*], A. Santos Silva [c], A. Hawreen [b,d]

[a] Department of Civil Engineering, School of Technology and Management, Polytechnic of Leiria, Campus 2 - Morro do Lena - Alto do Vieiro, P-4163-2411-901, Leiria, Portugal
[b] CERIS, Department of Civil Engineering, Architecture & Georresources, Instituto Superior Técnico, University of Lisbon, Av. Rovisco Pais, 1049-001, Lisbon, Portugal
[c] Department of Materials, National Laboratory for Civil Engineering, Avenida do Brasil, 101, P-1700-066, Lisbon, Portugal
[d] Department of Civil Engineering, Technical Engineering College, Erbil Polytechnic University, Kurdistan Region, Erbil, Iraq

ARTICLE INFO

Keywords:
ASR
CRA
Source concrete degradation
CRA properties

ABSTRACT

Knowing the aggregates' properties is fundamental for the correct design and performance prediction of concrete. The incorporation of coarse recycled aggregate (CRA) in concrete requires a deep understanding of CRA's capacity and limitations. CRA properties are mainly conditioned by the type of natural aggregates (NA), the interstitial transition zone (ITZ), and the adhered mortar's quality. All these conditions are restricted by the chemical, physical, and mechanical properties of the source concrete (SC). The potential alkali reactivity of CRA raises the alkali-silica reaction (ASR) issue when CRA incorporation in concrete is an option. The heterogeneity of CRA affects the reactive silica and alkali content present in NA and in the adhered mortar, respectively, depending on the characteristics of the SC. This makes it difficult to analyse the influence of CRA's heterogeneity when ASR-effected SC is used.

This work intends to investigate modifications of CRA properties due to ASR level in the SC. For this purpose, several tests including ASR evaluation, particle size distribution, density and bulk density, water absorption, shape index, flatness index and fragmentation resistance were performed on NA (fine and coarse) and CRA under natural and accelerated aging conditions. The results shown that the use of ASR-effected CRA does not change its mechanical and physical properties. In fact, these properties are more dependent on the corresponding characteristics of NA, ITZ, and the adhered mortar than on the ASR level in the SC.

1. Introduction

Reuse of construction and demolition waste (CDW), to minimize the demand and exploitation of natural resources, has become a reality. One of the methods to promote sustainable construction is incorporation of coarse recycled aggregates (CRA) in concrete.

Knowledge about the advantages and limitations of CRA is essential for the concrete mix design because CRA, in general, has more variable characteristics than coarse natural aggregates (CNA). CRA include CNA and fine natural aggregates (FNA), an interstitial transition zone (ITZ), and a portion of mortar adhered to them. These three interdependent constituents influence the properties of CRA and, in a second phase, change concrete's properties. In general, CRA presents higher porosity and water absorption than those of CNA of similar origin [1–3]. In comparison to CNA, CRA also shows a lower density, and crushing and abrasion resistance, usually depending on the content and quality of the adhered mortar [4–6].

Tavakoli and Soroushian [7] reported that the mechanical properties of CRA are influenced by the mechanical strength of the source concrete (SC), the ratio between coarse and fine aggregates in SC, the ratio between CNA maximum size in SC and CRA, the abrasion resistance of CRA, and the water absorption capacity of CRA.

Hansen and Narud [8] noted that the influence of the adhered mortar on concrete's performance increases with the reduction of CRA's grain size. Olorunsogo and Padayachee [9] observed that SC crushing creates cracks and voids in CRA that increase the penetration, diffusion, and absorption of liquids. Etxeberria [10] states that, if the same type of crusher and power were used, the amount of adhered mortar depends on

* Corresponding author.
E-mail addresses: miguel.santos@ipleiria.pt (M. Barreto Santos), jb@civil.ist.utl.pt (J. de Brito), ssilva@lnec.pt (A. Santos Silva), hawreen.a@gmail.com (A. Hawreen).

https://doi.org/10.1016/j.cemconcomp.2020.103621
Received 27 November 2019; Received in revised form 16 March 2020; Accepted 31 March 2020
Available online 8 April 2020

the aggregate size, the aggregate's resistant capacity, and the water/-cement (w/c) ratio of SC. Poon et al. [11] commented that the microstructural characteristics of ITZ in CRA is different from those found in CNA and are influenced by the properties of SC. Juan & Gutiérrez [12] found that the main constraints of CRA's quality are the amount of adhered mortar and the compressive strength of the SC. Rao et al. [5] reported that the fineness modulus of CRA was lower than that of CNA and the quantity of fine particles is essentially related to the crushing of concrete. Duan and Poon [6] indicated that good quality CRA, with a low adhered mortar and water absorption, can be used to replace CNA to produce a concrete with similar mechanical properties to concrete with only CNA.

However, in general, the physical and mechanical properties of CRA are lower than those of CNA. This is mainly due to the amount, porosity and strength of the adhered mortar and the effect of SC crushing on CRA's properties. The incorporation of CRA in concrete depends on full knowledge of their properties.

One of the concerns of the scientific community regarding the use of CRA is its potential reactivity to alkalis to promote alkali-silica reaction (ASR), one of the most damaging types of concrete degradation. Some natural aggregates (NA) can be potentially alkali reactive if they have sufficient amorphous content or disorganized silica constituents to react under certain humidity conditions with the alkalis of the concrete paste [13–15].

Nevertheless, references concerning CRA reactivity are frequently contradictory, regarding the effect of CRA on the occurrence of ASR. In general, standards regard CRA as a potentially reactive aggregate. Some studies have observed influence of aggregate crushing on its reactivity and variations on results caused by the amount of adhered mortar or water content [16–22].

However, CRA did not always show expansion in accelerated mortar or concrete expansion tests [10,23–25], which means that CRA is not always harmful related to ASR, probably due to age reactivity loss, amount of reactivity on NA used or alkali content. Barreto Santos et al. [26] confirmed that the use of CRA with non-reactive NA caused no remarkable expansion in concrete.

CRA is heterogeneous regarding the alkalis and reactive silica content, and it depends on the type of NA, and the type of SC and its exposure conditions. The knowledge and limitation of CRA's reactivity are very restrictive, compared with CNA, since it is quite difficult to control the origin of CRA. Several modified expansion tests have been studied to be an alternative to the mortar-bar and concrete prism tests used to detect the potential alkali-reactivity of NA, but the mentioned characteristics of CRA makes this process harder to perform [16,17,19–22].

ASR's inhibition is not restricted to removing the risk factor associated with the use of alkali-reactive aggregates. It is important to know the properties of CRA and of the reacting mechanism of ASR, and find ways to minimize the reaction effect, even when reactive aggregates are used.

In the present work, some SCs were produced with the objective of strictly controlling some of the uncertain properties of CRA and to know, in a first step, the effect of ASR on the mechanical and physical properties of CRA. For this purpose, controlled CRA were used (with alkali-reactive or non-reactive NA), which were subjected to different artificial aging regimes to simulate an old or newer structural concrete.

Density, water absorption and resistance to fragmentation are probably the CRA properties that are more affected by the ASR development on SC, mainly due to the adhered mortar. In this paper, these properties are presented. Changes in the physical and mechanical properties of CRA caused by the SC's state are commented. The aggregates were further characterized by particle size distribution, shape and flatness index, bulk density, the volume of voids and water absorption capacity over time. Tests were performed using the same procedure in CRA or CNA, to avoid entropies due to the used method.

2. Experimental program

2.1. Materials

CRA from a controlled SC was produced with CNA and FNA with known alkali-reactivity to limit the CRA's reactivity. The aggregates were separated according to their reactivity to alkalis. Alkali reactivity was evaluated by petrography [27] and by mortar and concrete expansion tests (accelerated mortar-bar test, [28]; concrete prism test RILEM AAR-3 [29].

Non-reactive SC (SC-nr) was produced with a limestone gravel (non-reactive coarse natural aggregate - CNA-nr) and a siliceous sand (non-reactive fine natural aggregate - FNA-nr). Reactive SC (SC-r) was produced with a reactive siliceous CNA (CNA-r) and a reactive siliceous FNA (FNA-r). The properties of aggregates are presented in Table 1. CEM I 42.5R was used in both concrete mix designs (Table 2). Two types of CNA were used, CNA1 and CNA2, with different size distributions. A CEM I 42.5R cement type with 0.86% sodium equivalent (Na_2O_{eq}) was used in both mixes (Table 2).

2.2. Concrete formulation and curing

Both SC-nr and SC-r were produced by a concrete company using the same procedure and composition, without alkali boosting. Mix design formulation included 680 kg/m^3 of FNA, 1220 kg/m^3 of CNA, and 364 kg/m^3 of cement. The average compressive strength of SC-nr and SC-r are 55 MPa and 65 MPa, respectively, at 28 days (Fig. 1). The 10 MPa difference between the SCs is attributed to the different types of NA used. Regarding tensile strength, the values at 28 days are similar.

After 6 months of SC production, water curing, cutting into blocks, and storage in boxes, a group of SC-nr and SC-r were exposed to accelerated aging in an environmental chamber (38 ± 2 °C and relative humidity > 95%) during 6 months to produce SC-nr-A and SC-*r*-A, respectively. The blocks were protected with plastic to minimize the calcium and alkalis lixiviation. These conditions are based on the recommendations of RILEM AAR-3 to study ASR using concrete prisms. Another group of SC-nr and SC-r were naturally aged outdoors during the same period to produce SC-nr-B and SC-*r*-B, respectively. After that, both SC groups were exposed for another 6 months to a natural exposure environment, stabilizing aging between both concrete mixes.

These two ageing groups were prepared to impose different levels of ASR development in SC-r and to study their influence on CRA's properties. ASR development was confirmed by observation using scanning electron microscopy with X-ray microanalysis (SEM/EDS).

After ageing, the different SC blocks were crushed and the obtained CRA were accordingly identified. Thus, the SC exposed to accelerated aging resulted in producing CRA-nr-A and CRA-*r*-A, while the natural aging SC resulted in producing CRA-nr-B and CRA-*r*-B.

CRA's particle size distribution and the concrete mix design were based on RILEM AAR-3 testing method [29]. The concrete mixes have 46% of coarse aggregate, by volume, at mass proportions of 30% of fine aggregates (0–4 mm), 30% of medium-sized aggregates (4–10 mm), and

Table 1
Natural aggregates base characteristics.

Aggregate	Dimension (d_{min}/D_{max}, mm)	Type	Form	ASR reactivity
CNA-nr2	11/22	Limestone	Crushed	Non-reactive
CNA-nr1	6/14	Limestone	Crushed	Non-reactive
CNA-r2	10/16	Siliceous	Crushed	High-reactive
CNA-r1	4/16	Siliceous	Crushed	High-reactive
FNA-nr	0/4	Siliceous	Round	Non-reactive
FNA-r	0/4	Siliceous	Round	Low-reactive

Legend: CNA = Coarse natural aggregates; FNA = Fine natural aggregates; nr = Non-reactive aggregates; r = Reactive aggregates; 1 = Smaller aggregates dimensions; 2 = Larger aggregates dimensions.

Table 2
Cement properties.

Cement type	Chemical analysis		Mechanical and physical analysis			
CEM 42.5R	Loss on ignition	2.77%		Days		
	SiO_2	19.31%		2d	7d	28d
	Al_2O_3	5.43%	Compression strength (MPa)	28.0	40.3	50.2
	Fe_2O_3	2.99%	Flexural strength (MPa)	5.2	6.7	7.6
	CaO total	63.62%	Density = 3.13 g/cm^3			
	MgO	1.64%	Expansibility = 1.5 g/cm^3			
	SO_3	2.80%				
	K_2O	1.11%	Setting time = 145 min.			
	CaO free	1.57%	Residue in the sieve 90 μm = 1.1%			
	Na_2O	0.13%				
	Na_2O_{eq}	0.86%				
CEM 52.5R	Loss on ignition	1.66%		Days		
	SiO_2	17.68%		2d	7d	28d
	Al_2O_3	5.28%	Compression strength (MPa)	38	48	–
	Fe_2O_3	3.22%	Flexural strength (MPa)	5.9	7.3	–
	CaO total	64.90%	Density = 3.10 g/cm^3			
	MgO	2.08%	Expansibility = 1.0 g/cm^3			
	SO_3	3.08%				
	K_2O	0.93%	Setting time = 130 min.			
	CaO free	2.69%	Residue in the sieve 90 μm = –%			
	Na_2O	0.13%				
	Na_2O_{eq}	0.74%				

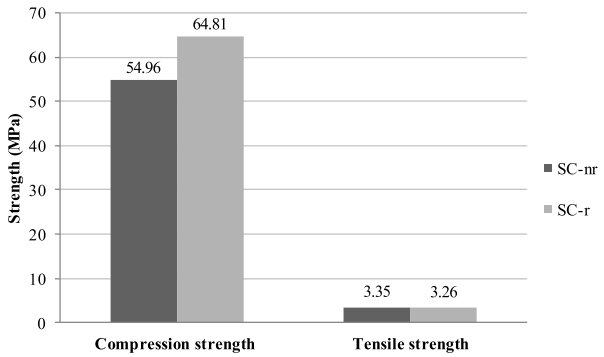

Fig. 1. Compressive and tensile strength of the source concrete.

40% of coarser aggregates (10–20 mm). An intermediate distribution of sizes 4–10 mm and 10–20 mm was taken by following a reference curve (limited by the overall percentages indicated by RILEM), using the graph of the Faury reference curves method as a base [30], with an aperture between sieves equal to the fifth root of the size of the aggregate. Each different type of aggregate, natural or recycled, was individually sieved in the d_{min}/D_{max} sizes given in Table 3, resulting in a conditioned particle size distribution. The apertures of the sieves are those of the base series plus series 2, provided in NP EN 12620 [31]. CNA and CRA thus had a matched particle size distribution, allowing their comparison.

2.3. Testing methods

The alkali-reactivity of NA was evaluated by petrographic analysis according to LNEC E415 [27] and by the accelerated mortar-bar test (AMBT) according to ASTM C1260 [28]. The reactivity of SC mixes was evaluated by the concrete prism test (CPT) as per the RILEM AAR-3 test-method (RILEM TC 106-AAR), without wrapping the prisms [32].

The mechanical and physical properties of aggregates (NA and RA) were characterized by the following tests: particle size distribution [33]; particle density and water absorption [34]; water absorption evolution over time [35]; bulk density and voids [36]; shape index [37]; flakiness index [38]; fragmentation resistance [39].

Table 3
Conditioned particle size distribution.

Particle size		Cumulative composition (Passing material)	Partial composition (Retained material)	
Dmax	Dmin	(%)	(% mass)	(% volume)
31.5	20	100.0	0.0	0.0
20	16	86.5	13.5	8.9
16	14	78.7	7.8	5.1
14	12.5	72.3	6.4	4.2
12.5	10	60.0	12.3	8.1
10	8	52.2	7.8	5.1
8	6.3	44.2	8.0	5.3
6.3	4	30.0	14.2	9.3
		Total:	70%	46%

3. Results and discussion

Table 4 summarizes the results of the geometric, physical and mechanical characterizations of NA used in the SC and RA. The geometric characterization was made by particle size analysis, shape index (SI), and flakiness index (FI). The physical properties included bulk density (ρ), void volume (v), apparent density (ρ_a), oven dry density (ρ_{rd}) and saturated surface dry density (ρ_{ssd}). The water absorption at 24 h (WA_{24}), and the percentage of water absorption of the aggregates with respect to their potential for absorbing over 5 min ($\%WA_{5m}$) were also assessed. The fragmentation test according to the Los Angeles method (LA) was performed for mechanical characterization.

3.1. ASR evaluation

A petrographic analysis shows that CNA-nr is a sedimentary carbonated rock. No forms of reactive silica minerals or potentially alkali suppliers were identified. CNA-r is composed of different types of siliceous rocks (Fig. 2), including quartzite, mylonite and gneiss. Deformed quartz grains and chert (reactive silica suppliers) and biotite, muscovite, chlorite and plagioclase (alkali supplier) are the main constituents.

AMBT confirms the reactivity of CNA-r, with an expansion average of 0.30 and 0.51% in CNA-r1 and 0.26 and 0.37% in CNA-r2, respectively at 14 and 28 days (Fig. 3). According to the expansion limits proposed in ASTM C 1260 (0.10% at 14 days), FNA-r and FNA-nr are both considered non-reactive to alkalis.

As mentioned before, the reactivity of concrete mixes was evaluated by CPT according to the RILEM AAR-3 test-method, without wrapping the prisms. SC was produced without any alkali boosting, as recommended in RILEM AAR-3 to achieve 5.5 kg of Na_2O_{eq}/m^3 of concrete. This change in alkali content of concrete has slowed down ASR's expansion.

The expansion results obtained in RILEM AAR-3 test confirm the results obtained by following ASTM C1260. After one year, SC-r reached a maximum expansion of 0.052%, which classifies it as potentially reactive. SC-nr showed a maximum expansion of 0.010% and was classified as non-reactive.

The accelerated ageing for six months was effective in the ASR development of SC-*r*-A, as further confirmed by SEM/EDS analysis (Fig. 4). On the other hand, the development of ASR in SC-*r*-B appears to be at an early stage (Fig. 5). As expected, SC-nr did not present any signs of deleterious ASR products (Figs. 6 and 7).

Table 4
Characterization of the source aggregates and conditioned mixtures.

Aggregates		d_{min}/D_{max} [mm]	ρ_a [kg/m^3]	ρ_{ssd} [kg/m^3]	ρ_{rd} [kg/m^3]	ρ [kg/m^3]	v [%]	WA_{24} [%]	$\%WA_{5m}$ [%]	SI [%]	FI [%]	LA [%]
Source aggregates	CNA-nr2	11/22	2720	2700	2680	1460	45.4	0.46	75	–	–	27
	CNA-nr1	6/14	2720	2700	2680	1490	44.4	0.48	75	–	–	28
	CNA-r2	10/16	2680	2650	2630	1410	45.8	0.62	75	–	–	19
	CNA-r1	4/16	2670	2630	2610	1400	46.6	0.76	75	–	–	24
	FNA-nr	0/4	2640	2630	2620	1450	44.7	0.26	50	–	–	–
	FNA-r	0/4	2650	2640	2630	1430	45.8	0.26	50	–	–	–
Conditioned mixture	CNA-nr	4/20	2720	2700	2680	1510	43.6	0.50	75	17	13.5	–
	CNA-r	4/20	2670	2640	2620	1440	44.9	0.63	75	21	13.4	–
	CRA-nr-A	4/20	2680	2540	2460	1320	46.2	3.26	80	24	13.7	41
	CRA-r-A	4/20	2650	2520	2440	1360	44.4	3.20	80	16	13.7	31
	CRA-nr-B	4/20	2680	2550	2470	–	–	3.10	80	–	–	36
	CRA-r-B	4/20	2660	2530	2450	1350	45.1	3.15	80	–	–	30

Legend: CNA = Coarse natural aggregates; FNA = Fine natural aggregates; CRA = Coarse recycled aggregates; nr = Non-reactive aggregates; r = Reactive aggregates; 1 = Smaller aggregates dimensions; 2 = Larger aggregates dimensions; A = Aggregates exposed to accelerated aging; B= Aggregates under natural aging; ρ_a = Apparent density; ρ_{rd} = Oven dry density; ρ_{ssd} = Saturated surface dry density; ρ = Bulk density; v = Void volume (v); WA_{24} = Water absorption at 24 h; WA_{5m} = Water absorption with respect to the potential to absorb over 5 min; SI = Shape index; FI = Flakiness index (FI); LA = Fragmentation resistance.

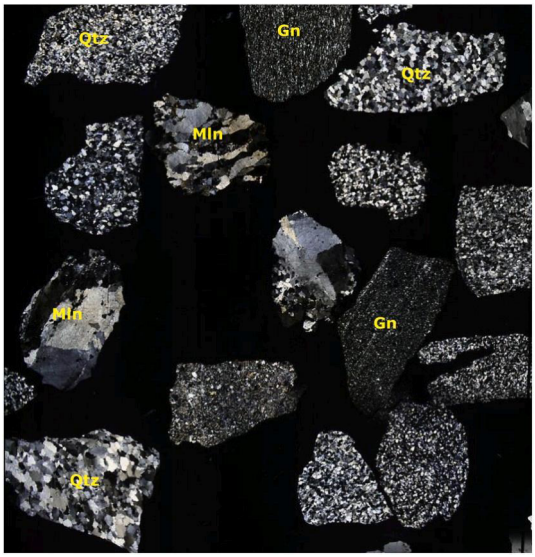

Fig. 2. Image of the CNA-r sample under polarized light microscope, showing fragments of quartzite (Qtz), milonites (Mln) and gneisses (Gn).

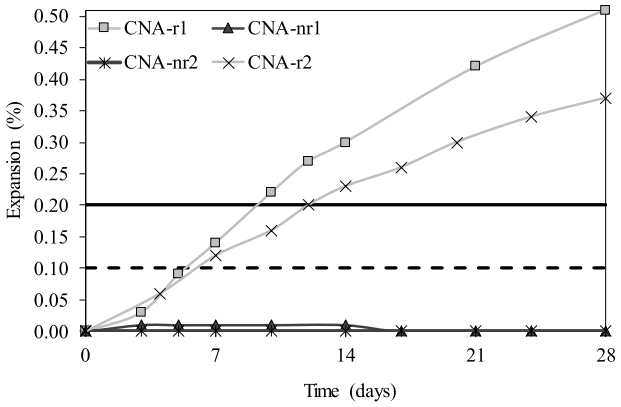

Fig. 3. Expansion test results CNA according to ASTM C 1260.

3.2. Particle size distribution

At the beginning of the CRA crushing process, several sieve analyses were performed to determine which jaw aperture (measured perpendicular to the jaw faces) was more effective to maximize the amount of intended coarse aggregates (4–20 mm range), which was found to be 5 mm. It is interesting to note that, for the same jaw opening, the grain size curves resulting from crushing the two SCs (SC-r and SC-nr), with different types of NA and tensile strength, were very similar (Fig. 8). The particle size distribution is uniform with the decrease of the jaw opening, resulting in a maximum difference of about 30% of material passed in the 16 mm sieve, between the jaw openings of 5 mm and 15 mm.

It was found that the same jaw opening of the crusher did not cause significant changes in the particle size distribution of CRA to:

- Different compressive strengths of SC (~10 MPa);
- Different CNA and FNA use, in the SCs tested;
- Different particle size distribution of the SCs tested.

Fig. 9 shows the original particle size distribution of each NA and the conditioned particle size distribution according to Table 3. A sample of each CRA and CNA has a conditioned particle size distribution to allow comparison.

3.3. Density and water absorption

Fig. 10 shows apparent density (ρ_a), oven dry density (ρ_{rd}), and saturated surface dry density (ρ_{ssd}). The results are indicated according to the particle size distribution and the type of aggregate .

It is observed that CNA with original particle size distribution have ρ_{ssd} between 2630 and 2700 kg/m^3. CNA with conditioned particle size distribution have values consistent with the applied mixture. Regardless of the SC type and ageing, CRA shows a decrease in ρ_{ssd}, when compared to that of CNA with the same conditioned particle size distribution. This decrease is more evident in ρ_a and ρ_{rd}. This difference is expected and is mainly due to the adhered mortar of CRA, which gives it a higher porosity and a lower density.

As mentioned, CRA is more porous than CNA. According to some authors [1–3], RA can absorb 3%–12% of water, depending on the size (fine or coarse) and SC properties. CNA and FNA had significantly lower water absorption values.

Fig. 11 shows the water absorption of the aggregates at 24 h (WA_{24}). There is a good correspondence between the values of water absorption indicated for CRA. WA_{24} of CRA was three times higher than that of

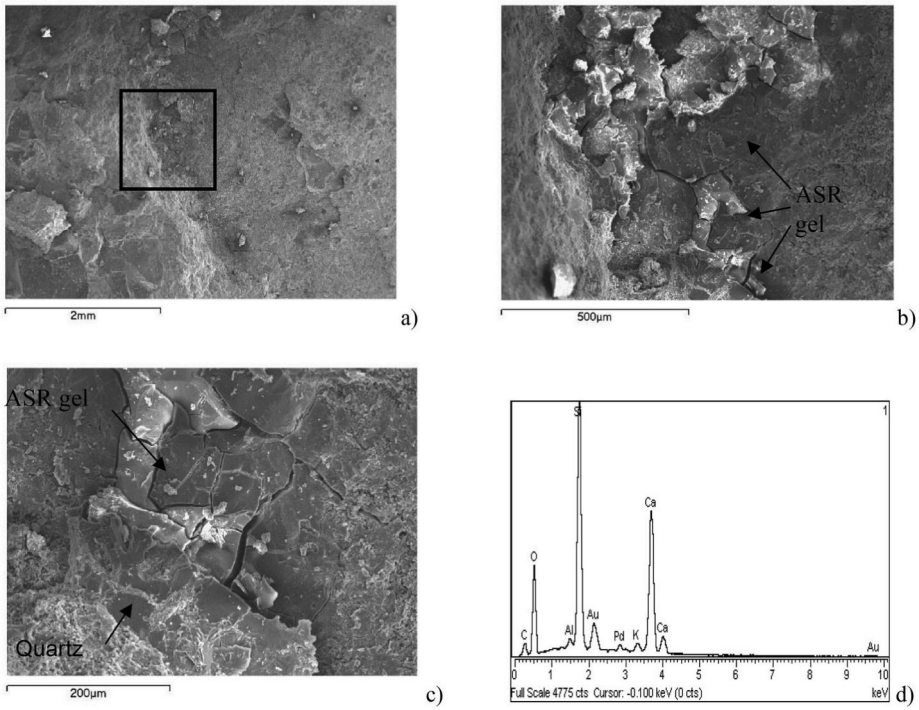

Fig. 4. SEM/EDS analysis of SC-*r*-A: a) General aspect of interface with ASR gel; b) Detail of marked zone a); c) Quartz interface with ASR gel; d) EDS spectrum of ASR gel.

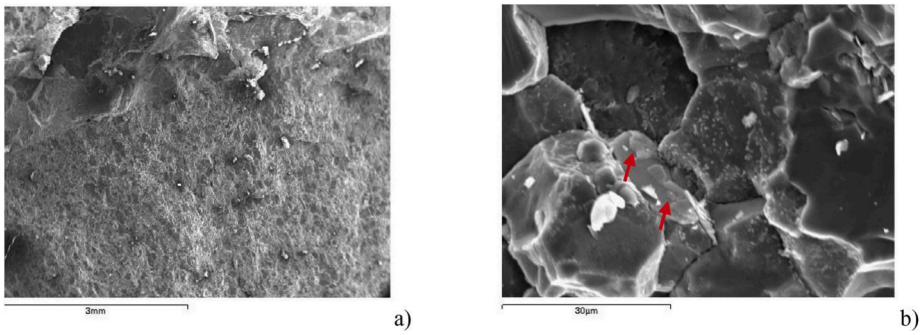

Fig. 5. SEM/EDS analysis of SC-*r*-B: a) Aspect of siliceous gravel; b) Detail of the grain boundaries, starting ASR gel formation (arrows).

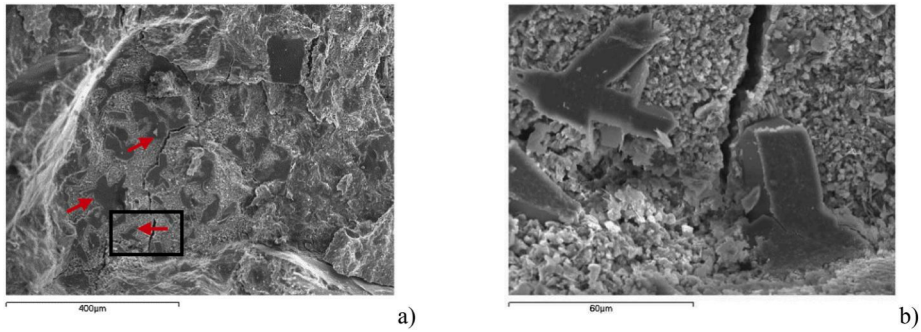

Fig. 6. SEM/EDS analysis of SC-nr-B: a) Interface with portlandite crystals (arrows); b) Detail of a).

CNA. Accelerated ageing caused a slightly higher water absorption (3.26%) than with natural ageing (3.10%); although consistent, it was insignificant and achieved a maximum difference of only 0.16% in CRA-nr-A. ASR of SC did not significantly affect the water absorption of the resulting CRA-*r*-A. Therefore, there was no noticeable influence of ASR development on the water absorption of CRA.

In CRA-nr and CNA-r, there was a tendency towards the increase of the water absorption with the decrease of the aggregates' density with the incorporation of different types of SC's aging (Fig. 12). It should be noted that, although the trend exists, the differences in values are small.

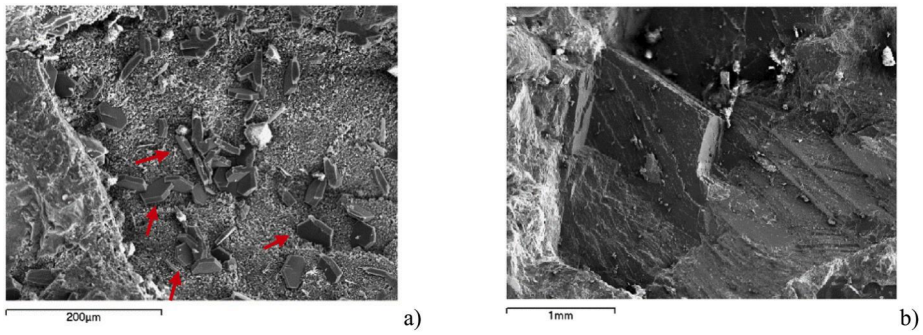

Fig. 7. SEM/EDS analysis of SC-nr-A: a) Portlandite crystals (arrows) on an interface zone; b) Limestone gravel grain, indicated by EDS.

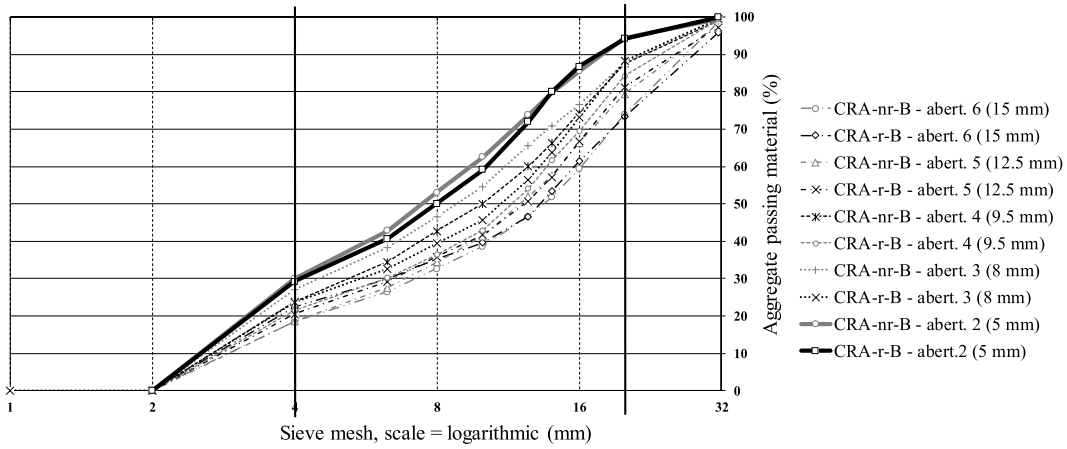

Fig. 8. Original particle size distribution of CRA sourced from SC-nr-B and SC-*r*-B.

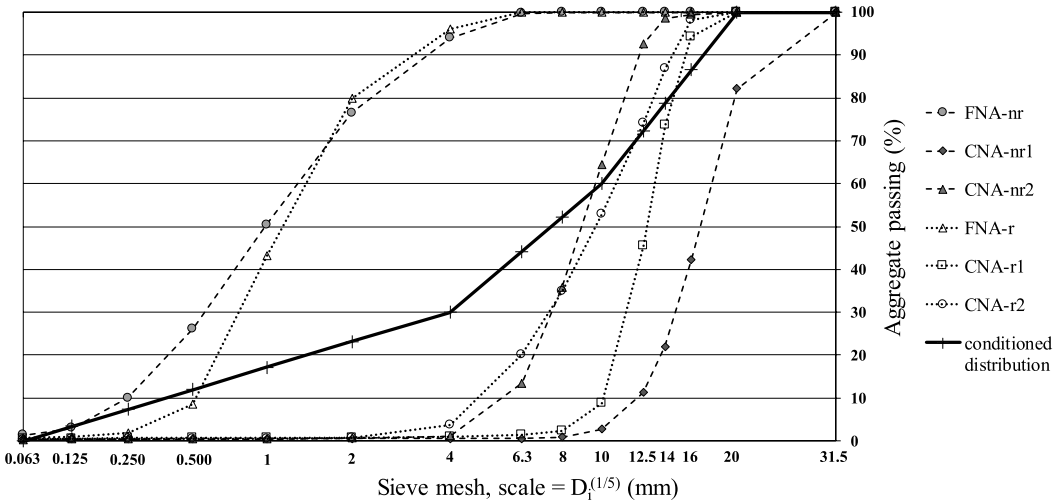

Fig. 9. Original particle size distribution of NA and conditioned particle size distribution used as a reference.

The aggregates' water absorption regarding their potential to absorb over 5 min (WA_{5m}) was also assessed. Water absorption over time is considered important when CRA's water absorption control is a concern to keep the effective w/c ratio of concrete mixes constant. Time of absorption depends on the mixing time of concrete. The analysis of the water absorption evolution over time was carried out based on the Ferreira et al. [35] method, using a hydrostatic weight balance. The pycnometer method was also used to compare methods.

Methods comparison was performed using CRA-nr-A and CRA-*r*-A (Fig. 13). In the first minutes, there were no significant differences between the water absorption evolutions of the aggregates according to the methods used. After 16 min, the pycnometer method presented lower values of water absorption relative to the potential absorption. There were no significant differences between the water absorption evolutions of CRA. CRA absorbed 75–80% of their potential water absorption, at 5 min as shown in the shading in Fig. 13.

The stronger shake of the pycnometer may have minimized the number of air bubbles between the particles, accelerating water absorption in the first few minutes. The use of the metal mesh basket did not prevent the loss of some fine particles aggregated to the CRA, which

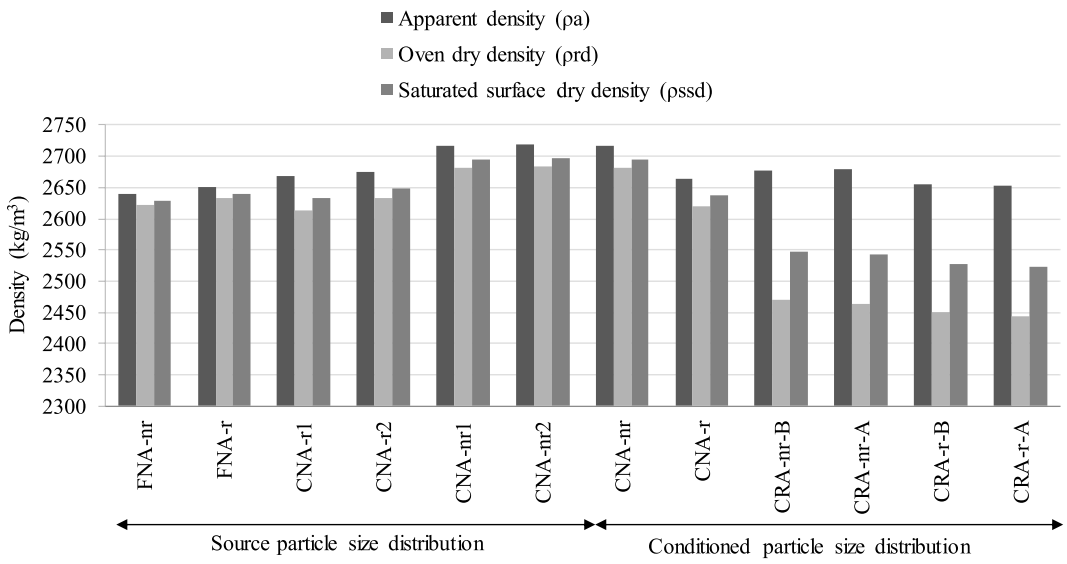

Fig. 10. Density of CNA and CRA

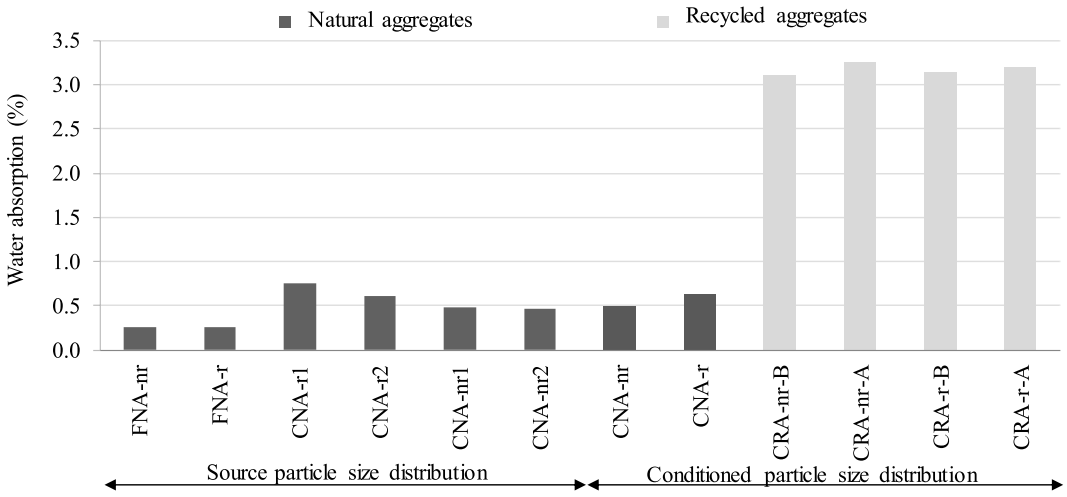

Fig. 11. Water absorption of CNA and CRA.

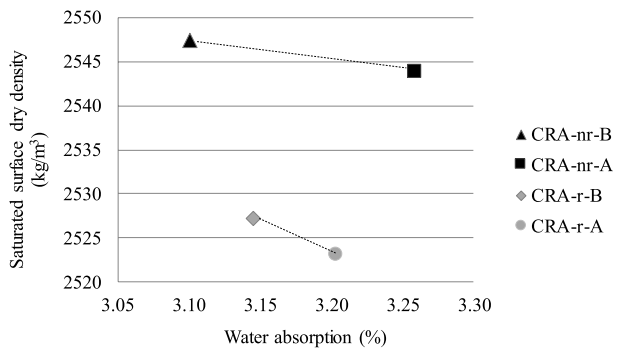

Fig. 12. Relation between the saturated surface dry density of CRA and their capacity of water absorption, according to the type of SC aging.

may have also changed the water absorption values relative to their potential absorption, due to the mass loss of the sample. However, both methods appeared to be effective in determining the water absorption evolution of aggregates over time.

CNA absorbed between 70% and 75% of their potential water absorption (Fig. 14). The water absorption of FNA was slower, only about 50% of the potential absorption. The water absorption values of CNA and FNA were very low (<0.8%). However, the water absorption speed over time in CNA was similar to that of CRA.

3.4. Bulk density

Fig. 15 shows the results of bulk density (ρb) and the volume of voids (v) of CRA, CNA and FNA. The results confirmed the lower bulk density of CRA than CNA. The bulk densities of CNA and CRA were 1400–1510 kg/m^3 and 1320–1360 kg/m^3, respectively. The void volume did not show any clear trend between CNA and CRA, which was remarkable because it is more dependent on the particle size distribution and particle adjustment than on physical characteristics. The volume of voids of all type of aggregates was between 44% and 47%.

There was a decrease in the bulk density of CNA with the original particle size distribution when compared to that of CNA with conditioned particle size distributions. This was evidenced by the higher void volume of CNA with the original distribution. CRA, regardless of the SC type or aging, presented a decrease in bulk density when compared to that of CNA with corresponding conditioned particle size distribution.

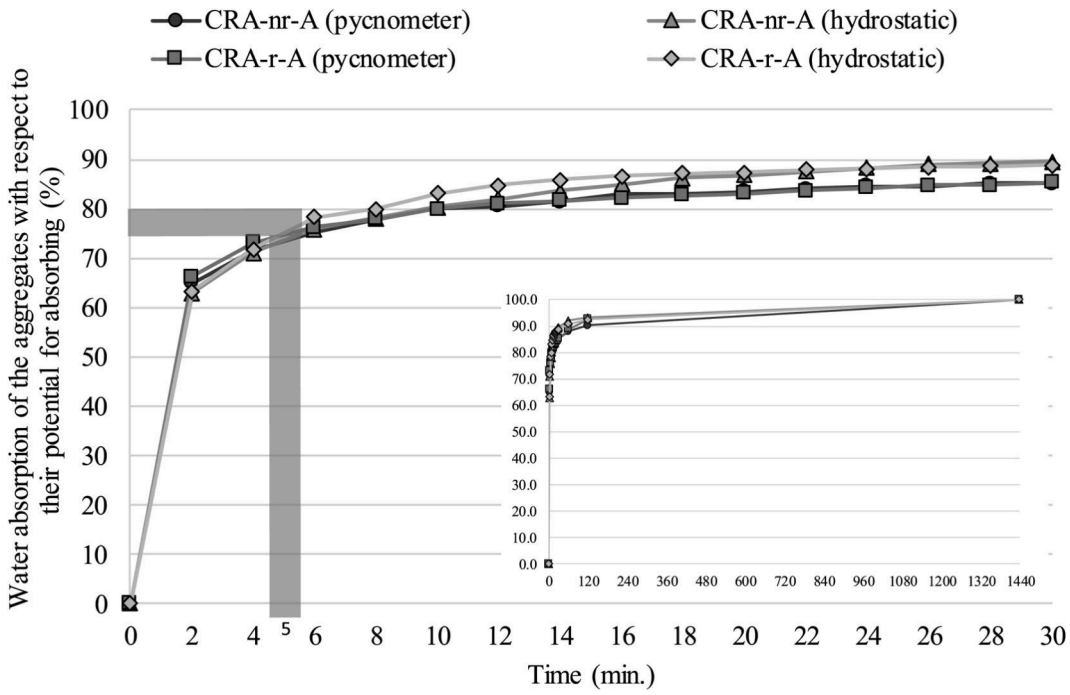

Fig. 13. Water absorption evolution of CRA up to 30 min. The inset graph shows the absorption evolution up to 24 h.

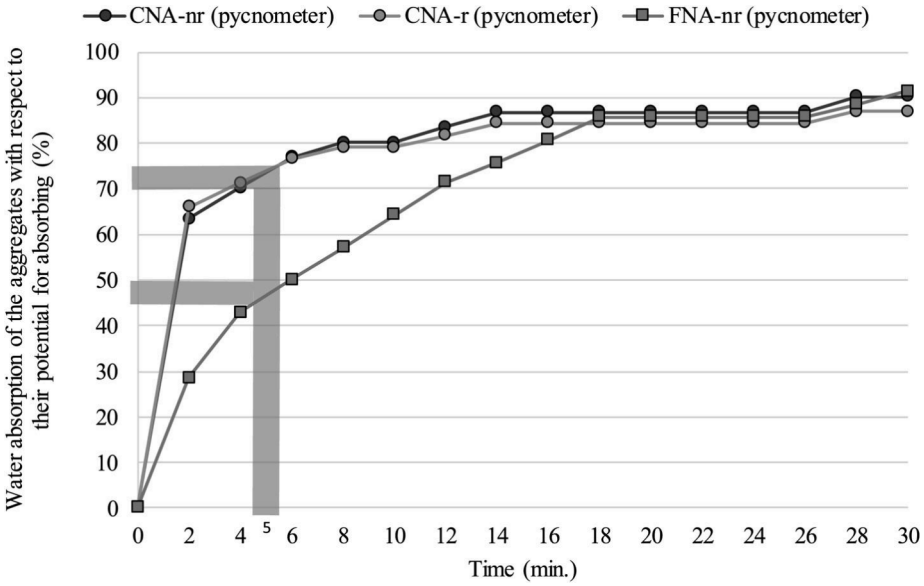

Fig. 14. Water absorption evolution of CNA and FNA up to 30 min.

This discrepancy is expected and is mainly due to the adhered mortar of CRA.

3.5. Shape and flakiness index

The shape index (SI) relates the length and thickness of the particles. As shown in Table 4, CNA-r have the most elongated particles. The opposite behaviour can be seen for CRA. Fonseca et al. [40] obtained SI of 24% in CRA produced from SC with 40 MPa. Silva et al. [41] observed that the type of crusher used and the number of successive crushing influence the shape and size of the aggregates.

CRA of the present study were produced with the same crusher, using the same jaw opening and only one primary crushing. The lower mechanical strength of SC-nr seems to justify the formation of more elongated particles. The SI of CNA used in SC did not have a significant influence on the SI of the produced CRA.

The test to determine the flakiness index (FI) consists of passing a set of aggregate size fractions through a defined group of corresponding bar sieves, thus evaluating the more or less flattened shape of the particles. In Table 4, the FI results of the conditioned particle size distribution aggregates are presented. Fig. 16 shows the individual FI of each fraction (FI_i).

The results suggest the analysed aggregates have a quite similar FI, between 13% and 14%. However, FI_i presented significant differences. For example, there is a 10% difference in 5/6.3 dimension between CNA-nr and CNA-r, with flakiness particles in this CNA-r dimension. The opposite behaviour was observed in the 4/5 range, with CNA-nr having a higher FI. CRA-r and CRA-nr had closer FI_i values.

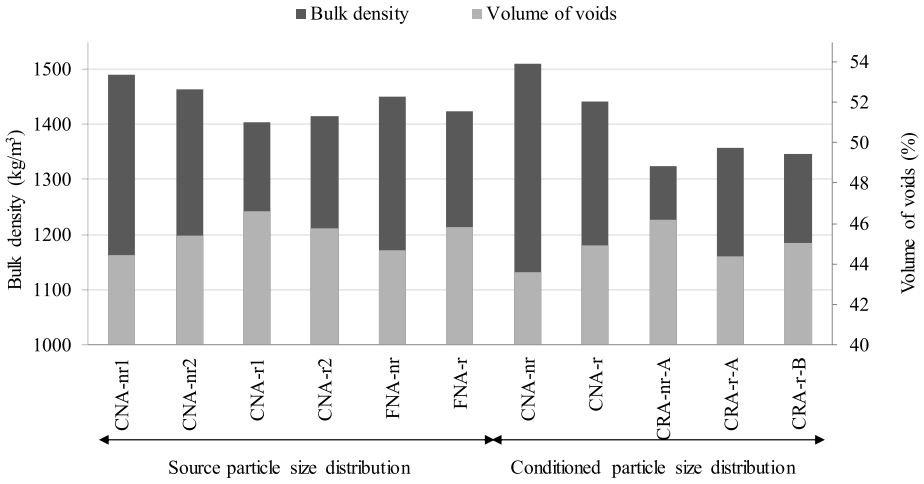

Fig. 15. Bulk density and void volume of CNA, FNA and CRA.

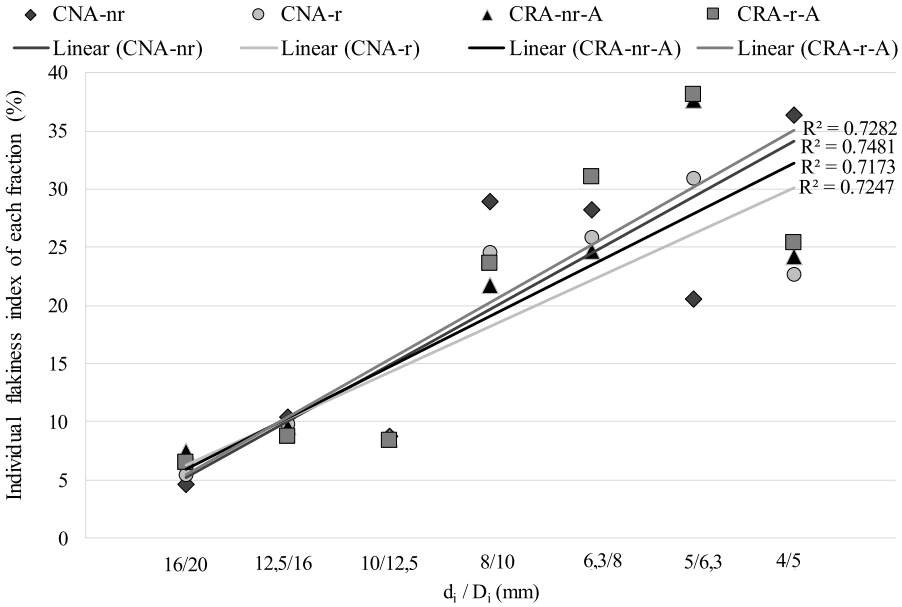

Fig. 16. Flakiness index of CNA and CRA.

The results show that there is not a clear difference between FI of CNA and CRA. However, with some dispersion, the trend lines of Fig. 16 show that particle flakiness decreases with grain size reduction.

3.6. Fragmentation resistance

The Los Angeles coefficient (LA) allows analysing the resistance to fragmentation of the aggregates and indirectly predicting their mechanical strength. According to NP EN 1097–2 [39], for each type of aggregate, a sample with 35% of the material with 12.5/14 size and 65% of the material with 10/12.5 size were considered.

In this study, the LA coefficient values of CNA are between 19% and 28% (Fig. 17). These values increased in the case of CRA to 30–41%. There is still a slight decrease in CRA from SC with accelerated aging. Between CRA and CNA, the decrease in LA coefficient is consistent, with an average reduction of 42%.

The lower resistance to fragmentation of RA compared to NA, reached in the study, is in agreement with similar studies referred in the literature. Hansen and Narud [8] reported that LA abrasion loss values of RA were 20–50% higher than those of NA. Tabsh and Abdelfatah [4]

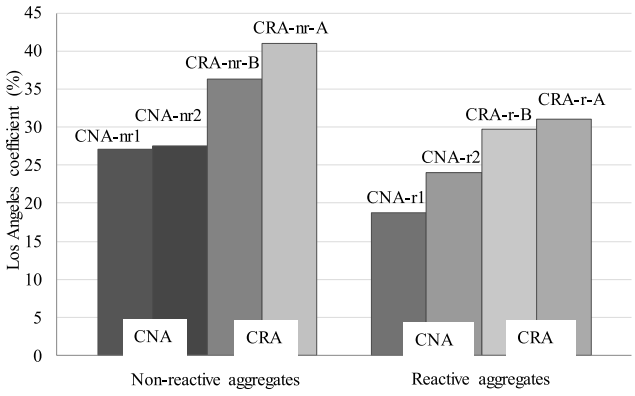

Fig. 17. Fragmentation resistance of CNA and CRA.

obtained an average increase of 30% in LA coefficient of RA compared to that of NA, associated with the mechanical strength of the SC. In the same study, a reduction of 37% in LA was observed when RA of older and lower quality SC was used. As mentioned in the introduction, Juan & Gutiérrez [12] suggested the limitation of RA use from SC with at least 25 MPa of compressive strength and a maximum limit of 44% of adhered mortar to obtain good quality RA.

4. Conclusions

The properties of CRA, with focus on those considered to be the most conditioned in the future by the development of ASR in SC, were studied in this paper. The main conclusions of the results analysis are the following:

- The density and water absorption of CRA were slightly influenced by the type of SC, the type of CNA and FNA used in SC, and the type of SC ageing.
- The individual flakiness index of CRA and CNA significantly increased with the reduction of their particles size, although these had a reduced overall flakiness index.
- There was some elongation of the CRA-nr particles relative to CRA-r, probably due to the 10 MPa lower mechanical strength of SC-nr.
- The fragmentation resistance had a general decrease in the LA coefficient of CRA when compared to CNA.
- The adhered mortar appeared to be the reason for the values achieved in CRA's properties, since SC were produced with the same composition, differing only in the type of NA used;
- ASR development in SC did not have a marked influence on CRA's properties.

Declaration of competing interest

The authors declare that they have no known competing financial interests or personal relationships that could have appeared to influence the work reported in this paper.

Acknowledgments

The authors gratefully acknowledge the support of CERIS (Civil Engineering Research and Innovation for Sustainability), FCT (Foundation for Science and Technology), and LNEC (National Laboratory for Civil Engineering) for their support through the project RE-IMPROVE (Expansive reactions in concrete - Prevention and mitigation of their effects).

References

[1] J.M. Gomez-Sobéron, Porosity of recycled concrete with substitution of recycled concrete aggregate - an experimental study, Cement Concr. Res. 32 (2002) 1301–1311.
[2] A. Katz, Properties of concrete made with recycled aggregate from partially hydrated old concrete, Cement Concr. Res. 33 (2003) 703–711.
[3] A. Rao, K. Jha, S. Misra, Use of aggregates from recycled construction and demolition waste in concrete, Resour. Conserv. Recycl. 50 (2007) 71–81.
[4] S.W. Tabsh, A.S. Abdelfatah, Influence of recycled concrete aggregates on strength properties of concrete, Construct. Build. Mater. 23 (2009) 1163–1167.
[5] M. Rao, S.K. Bhattacharyya, S.V. Barai, Influence of field recycled coarse aggregate on properties of concrete, Mater. Struct. 44 (2011) 205–220.
[6] Z.H. Duan, C.S. Poon, Properties of recycled aggregate concrete made with recycled aggregates with different amounts of old adhered mortars, Mater. Des. 58 (2014) 19–29.
[7] M. Tavakoli, P. Soroushian, Strengths of recycled aggregate concrete made using field-demolished concrete as aggregate, ACI Mater. J. 93 (2) (1997) 178–181.
[8] T. Hansen, H. Narud, Strength of recycled concrete made from crushed concrete coarse aggregate, Concr. Int. 5 (1) (1983) 79–83.
[9] F.T. Olorunsogo, N. Padayachee, Performance of recycled aggregate concrete monitored by durability indexes, Cement Concr. Res. 32 (2002) 179–185.
[10] M. Etxeberria, Experimental Study on Microstructure and Structural Behaviour of Recycled Aggregate Concrete, Doctoral thesis in Civil Engineering, Polytechnic University of Catalonia, Barcelona, March, 2004.
[11] C.S. Poon, L. Shui, L. Lam, Effect of microstructure of ITZ on compressive strength of concrete prepared with recycled aggregates, Construct. Build. Mater. 18 (2004) 461–468.
[12] M. de Juan, P.A. Gutiérrez, Study on the influence of attached mortar content on the properties of recycled concrete aggregate, Construct. Build. Mater. 23 (2009) 872–877.
[13] D.W. Hobbs, Alkali-silica Reaction in Concrete, Thomas Telford Ltd., UK, 1988.
[14] R.N. Swamy, The Alkali-Silica Reaction in Concrete, CRC Press, UK, 1992.
[15] I. Sims, A.B. Poole, Alkali-aggregate Reaction in Concrete: A World Review, CRC Press, UK, 2017.
[16] D.L. Gress, R.L. Kozikowski, Accelerated ASR testing of concrete prisms incorporating recycled concrete aggregate, in: Proceedings of the 11th International Conference on Alkali-Aggregate Reaction in Concrete, ICAAR, Quebec City, Canada, 2000, pp. 1139–1148.
[17] I.V.H.C. Scott, Mitigating Alkali Silicate Reaction in Recycled Concrete, Master Thesis in Civil Engineering, New Hampshire University, United States, 2006.
[18] M. Shehata, C. Christidis, W. Mikhaiel, C. Rogers, M. Lachemi, Reactivity of reclaimed concrete aggregate produced from concrete affected by alkali–silica reaction, Cement Concr. Res. 40 (4) (2010) 575–582.
[19] M. Adams, B. Gray, J. Ideker, J. Tanner, A. Jones, B. Fournier, S. Beauchemin, M. Shehata, R. Johnson, Applicability of standard alkali-silica reactivity testing methods for recycled concrete aggregate, in: Proceedings of the 14th International Conference on Alkali-Aggregate Reaction in Concrete, ICAAR, Austin, United States, 2012.
[20] R. Johnson, M. Shehata, The efficacy of accelerated test methods to evaluate alkali silica reactivity of recycled concrete aggregates, Construct. Build. Mater. 112 (2016) 518–528.
[21] F. Delobel, D. Bulteel, J.M. Mechling, A. Lecomte, M. Cyr, S. Rémond, Application of ASR tests to recycled concrete aggregates: influence of water absorption, Construct. Build. Mater. 124 (2016) 714–721.
[22] S. Beauchemin, B. Fournier, J. Duchesne, Evaluation of the concrete prisms test method for assessing the potential alkali-aggregate reactivity of recycled concrete aggregates, Cement Concr. Res. 104 (2018) 25–36.
[23] J. Desmyter, S. Blockmans, Evaluation of different measures to reduce the risk of alkali-silica reaction in recycled aggregate concrete, in: June, Quebec City, Canada Proceedings of the 11th International Conference on Alkali-Aggregate Reaction in Concrete, ICAAR, 2000, pp. 603–612.
[24] A.J. Calder, M. McKenzie, The Susceptibility of Recycled Concrete Aggregate to Alkali Silica Reaction, Transport Research Laboratory, UK, 2005. Published Project Report PPR037.
[25] R.K. Dhir, M.J. McCarthy, J.E. Halliday, M.C. Tang, ASR Guidance on Recycled Aggregates - Guidance on Alkali Limits and Reactivity. DTI/WRAP Aggregates Research Programme STBF 13/14C, The Waste and Resources Action Programme, 2005.
[26] M. Barreto Santos, A. Santos Silva, J. de Brito, ASR impact on concrete with recycled aggregates, in: Proceedings of the 15th International Conference on Alkali-Aggregate Reaction in Concrete, ICAAR, São Paulo, Brazil, 2016.
[27] LNEC E 415, Aggregates for Mortar and Concrete. Determination of the Potential Reactivity with the Alkalis. Petrographic Examination, National Laboratory for Civil Engineering, 1993 (in Portuguese).
[28] ASTM C 1260 Standard Test Method for Potential Alkali Reactivity of Aggregates (Mortar Bar Method), The American Society for Testing and Materials, 2012.
[29] RILEM TC 106-AAR, Alkali-aggregate reaction: recommendations, Mater. Struct. 33 (2000) 283–293.
[30] J.P. Faury, Le Béton (In French), Dunod, Paris, France, 1958.
[31] NP EN 12620, Aggregates for Concrete, Portuguese Standard, IPQ, 2004.
[32] RILEM, Recommendations for the prevention of damage by alkali-aggregate reactions in new concrete structures - state-of-the-art report of the RILEM Technical Committee 219-ACS, in: P.J. Nixon, I. Sims (Eds.), RILEM State-Of-The-Art Reports, Springer, 2016, p. 168.
[33] NP EN 933-1, Tests for Geometrical Properties of Aggregates - Part 1: Determination of Particle Size Distribution – Sieving Method, Portuguese Standard, IPQ, 2000.
[34] NP EN 1097-6, Tests for Mechanical and Physical Properties of Aggregates - Part 6: Determination of Particle Density and Water Absorption, Portuguese Standard, IPQ, 2003.
[35] L. Ferreira, J. de Brito, M. Barra, Influence of the pre-saturation of recycled coarse concrete aggregates on concrete properties, Mag. Concr. Res. 63 (8) (2011) 617–627.
[36] NP EN 1097-3, Tests for Mechanical and Physical Properties of Aggregates - Part 3: Determination of Loose Bulk Density and Voids, Portuguese Standard, IPQ, 2002.
[37] NP EN 933-4, Tests for Geometrical Properties of Aggregates - Part 4: Determination of Particle Shape - Shape Index, Portuguese Standard, IPQ, 2002.
[38] NP EN 933-3 Tests for geometrical properties of aggregates, Part 3: Determination of Particle Shape - Flakiness Index, Portuguese Standard, IPQ, 2002.
[39] NP EN 1097-2, Tests for Mechanical and Physical Properties of Aggregates - Part 2: Methods for the Determination of Resistance to Fragmentation, Portuguese Standard, IPQ, 2002.
[40] N. Fonseca, J. de Brito, L. Evangelista, The influence of curing conditions on the mechanical performance of concrete made with recycled concrete waste, Cement Concr. Compos. 33 (6) (2011) 637–643.
[41] R.V. Silva, J. de Brito, R.K. Dhir, Properties and composition of recycled aggregates from construction and demolition waste suitable for concrete production, Construct. Build. Mater. 65 (2014) 201–217.

Update

Cement and Concrete Composites
Volume 114, Issue , November 2020, Page

DOI: https://doi.org/10.1016/j.cemconcomp.2020.103778

Cement and Concrete Composites 114 (2020) 103778

Contents lists available at ScienceDirect

Cement and Concrete Composites

journal homepage: http://www.elsevier.com/locate/cemconcomp

Corrigendum to "Effect of the source concrete with ASR degradation on the mechanical and physical properties of coarse recycled aggregate" [Cement Concr. Compos. (2020) 103621]

M. Barreto Santos [a], J. de Brito [b,*], A. Santos Silva [c], A. Hawreen [b,d]

[a] Department of Civil Engineering, School of Technology and Management, Polytechnic of Leiria, Campus 2 - Morro do Lena - Alto do Vieiro, P-4163-2411-901, Leiria, Portugal
[b] CERIS, Department of Civil Engineering, Architecture & Georesources, Instituto Superior Técnico, University of Lisbon, Av. Rovisco Pais, 1049-001, Lisbon, Portugal
[c] Department of Materials, National Laboratory for Civil Engineering, Avenida do Brasil, 101, P-1700-066, Lisbon, Portugal
[d] Department of Civil Engineering, Technical Engineering College, Erbil Polytechnic University, Kurdistan Region, Erbil, Iraq

The authors regret Dear members of Cement and Concrete Composites Journal, I (A. Hawreen) have recently published a paper in your journal under the title "Effect of the source concrete with ASR degradation on the mechanical and physical properties of coarse recycled aggregate". If it is possible, I would like update my affiliation as shown below:

Author name: A. Hawreen.

Author email: hawreen.a@gmail.com.

First affiliation: Department of Civil Engineering, Technical Engineering College, Erbil Polytechnic University, Kurdistan Region, Erbil, Iraq.

Second affiliation: Scientific Research and Development Center, Nawroz University, Duhok, Kurdistan-Region, Iraq.

Please consider the two mentioned affiliations in order (one after another).

I look forward to hearing from you.

Best regards,

A. Hawreen.

The authors would like to apologise for any inconvenience caused.

DOI of original article: https://doi.org/10.1016/j.cemconcomp.2020.103621.

* Corresponding author.
E-mail address: jb@civil.ist.utl.pt (J. de Brito).

https://doi.org/10.1016/j.cemconcomp.2020.103778

Available online 10 September 2020